Sensors and Materials, Vol. 38, No. 2 (2026) 545–551
MYU Tokyo

S & M 4319

Scintillation Properties of Sr-admixed Ce-doped $CaHfO_3$ Single Crystals

Hiroyuki Fukushima,[1*] Daisuke Nakauchi,[2] Takumi Kato,[2]
Noriaki Kawaguchi,[2] and Takayuki Yanagida[2]

[1]Department of Electrical and Electronic Engineering, National Institute of Technology, Fukui College, Geshi, Sabae, Fukui 916-8507, Japan
[2]Division of Materials Science, Nara Institute of Science and Technology, 8916-5 Takayama-cho, Ikoma, Nara 630-0192, Japan

(Received October 31, 2025; accepted December 22, 2025)

Keywords: photoluminescence, radioluminescence, Ce ion, $CaHfO_3$, single crystal

Sr-admixed Ce:$CaHfO_3$ single crystals were synthesized by the floating zone method, and their photoluminescence and scintillation properties were investigated. The 5d–4f transition of Ce^{3+} exhibited blue luminescence at around 430 nm with the fast decay time in the 20 ns range. The maximum quantum yield of Sr-admixed Ce:$CaHfO_3$ was 57%. In scintillation, Sr-admixed Ce:$CaHfO_3$ showed bright luminescence. The maximum light yield was 2880 photons/MeV with low afterglow.

1. Introduction

Scintillators have been used to indirectly detect ionizing radiation. When scintillators absorb the energy of the ionizing radiation, they emit luminescence, which is converted to electric signals using photodetectors such as photomultiplier tubes or photodiodes. The typical wavelength sensitivity of a photomultiplier tube is the UV to blue region; thus, the common scintillators exhibit blue luminescence using luminescence centers such as Tl^+ or Ce^{3+}.[1–5] To develop novel scintillators, many materials in the form of single crystals,[6–19] ceramics,[20–23] and glasses[24–30] have been investigated.

Ce:$CaHfO_3$ is a candidate for the novel X- or γ-ray detection scintillator owing to its high density (6.9 g/cm^3) and effective atomic number (65). The light yield of Ce:$CaHfO_3$ is 7800 photons/MeV under ^{137}Cs γ-ray irradiation, and the decay time constant is 20 ns.[31] The fast decay time is advantageous for photon-counting applications. However, the mediocre light yield should be increased to use Ce:$CaHfO_3$ in applications. Furthermore, the afterglow level of Ce:$CaHfO_3$ is quite high. The high afterglow level is inappropriate for applications. To improve these properties, Mg-admixed Ce:$CaHfO_3$ has been investigated.[32] The light yield is increased to 9500 photons/MeV under ^{137}Cs γ-ray irradiation although the afterglow level is high. A possible reason for the high afterglow level is the imperfect incorporation of Mg into Ca. The

*Corresponding author: e-mail: fukushima@fukui-nct.ac.jp
https://doi.org/10.18494/SAM6082

ISSN 0914-4935
https://myukk.org/

coordination number of Ca in $CaHfO_3$ is 12, although the maximum coordination number of Mg is 8.[33] When Mg^{2+} is substituted to the Ca^{2+} site in the $CaHfO_3$ composition, the bonding state around Mg^{2+} is imperfect compared with a normal $CaHfO_3$. Such imperfection may lead to defects and a high afterglow level. From these reasons, Sr admixture in Ce:$CaHfO_3$ is meaningful to reduce the afterglow level in Ce:$CaHfO_3$ because the elemental properties of both Ca and Sr are similar, and the maximum coordination number of Sr^{2+} is 12. In this study, Sr-admixed Ce:$CaHfO_3$ single crystals were synthesized by the floating zone method, and the photoluminescence (PL) and scintillation properties were investigated.

2. Materials and Methods

Sr-admixed Ce:$CaHfO_3$ single crystals were synthesized by the floating zone method. CaO (99.99%), $SrCO_3$ (99.99%), HfO_2 (99.95%), and CeO_2 (99.99%) powders were used to make feed rods. The nominal concentration of Ce was fixed to 3 mol.% because the optimum concentration of Ce in the Mg-admixed Ce:$CaHfO_3$ was 3 mol.%.[32] The amounts of Sr with respect to the Ca site were 0.5, 2.5, 5, and 10 mol.%. The reason for the high admix concentration is to compensate for the volatilization of Ca during the crystal growth. These powders were weighed using an electric scale and mixed homogeneously using a mortar and a pestle. To avoid Ca deficiency in crystals, 10 mol.% CaO was added from a stoichiometric composition. The condition of the single crystal growth was reported in a previous study.[31] The X-ray diffraction (XRD) patterns were measured in the range of 10–70º (Rigaku, MiniFlex600). The PL emission and excitation map, as well as quantum yield (QY), was measured with a spectrometer (Hamamatsu Photonics, C11347). The PL decay curve was also measured with a spectrometer (Hamamatsu Photonics, C11367). The radioluminescence spectra and decay curves were recorded using a laboratory-made setup.[34,35] The pulse height distribution was measured in the same manner as previously reported.[34] The ^{137}Cs γ-ray (662 keV) was used as an irradiation source. The reference crystal was Ce:Gd_2SiO_5 with the light yield of 7000 photons/MeV. The shaping time was 2 μs.

3. Results and Discussion

The XRD patterns and appearance of the samples are shown in Fig. 1. The obtained XRD patterns agreed with the reference XRD pattern of $CaHfO_3$ (ICDD. 36-1473). No impurity phases were detected in this measurement. The appearance of the samples was colorless and transparent. The peak position was slightly shifted to a lower angle. The ionic radii of Ca^{2+} and Sr^{2+} in 12-coordination were 1.34 and 1.44 Å, respectively.[33] On the basis of these results, the added Sr was incorporated into the Ca site, and the synthesized samples were a single phase of $CaHfO_3$.

As illustrated in Fig. 2, the PL emission and excitation map of a 0.5% Sr-admixed Ce:$CaHfO_3$ single crystal is presented as a representative result. The horizontal and vertical axes are emission and excitation wavelengths, respectively. The intensity is presented by the color. The broad luminescence band was observed at around 430 nm under the excitation wavelength at around 340 nm. The spectral feature was similar to the previously reported PL spectra of

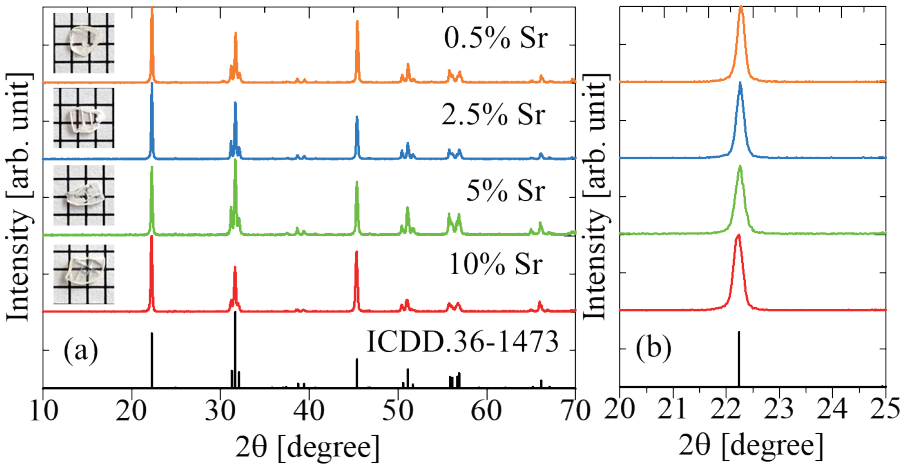

Fig. 1. (Color online) (a) XRD patterns and appearance of samples. (b) Enlarged XRD patterns.

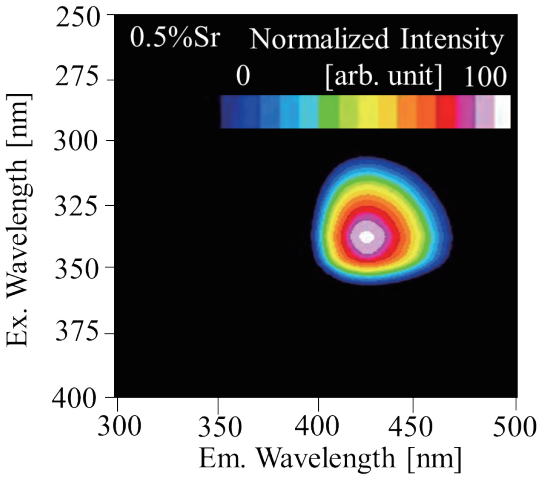

Fig. 2. (Color online) PL emission and excitation map of 0.5% Sr-admixed Ce:$CaHfO_3$ single crystal.

Ce:$CaHfO_3$.[31,36] The PL QYs of 0.5, 2.5, 5, and 10% Sr-admixed Ce:$CaHfO_3$ were 57, 56, 44, and 38%, respectively. These values were higher than those of Ce:$CaHfO_3$ and Mg-admixed Ce:$CaHfO_3$.[31,32] Figure 3 shows the PL decay curves of Sr-admixed Ce:$CaHfO_3$ single crystals. The excitation and monitoring wavelengths were 340 and 430 nm, respectively. The PL decay curves were fitted with a single exponential component. The PL decay constants of 0.5, 2.5, 5, and 10% Sr-admixed Ce:$CaHfO_3$ were 23.4, 23.3, 22.7, and 21.1 ns, respectively. The origin of luminescence was identified as the 5d–4f transition of Ce^{3+}, taking into account the observed spectral features and decay time constants. The PL QYs and decay constants decreased with increasing Sr concentration. Consequently, an increase in the Sr concentration led to a decrease in the radiative rate constants and an increase in the nonradiative rate constants.

Figure 4 shows the radioluminescence spectra of Sr-admixed Ce:$CaHfO_3$ single crystals. A broad luminescence band at around 430 nm was observed. The luminescence feature was similar

to that observed in PL and a previous study.[31] Figure 5 shows the radioluminescence decay curves of Sr-admixed Ce:$CaHfO_3$ single crystals. These decay curves were fitted with the sum of two exponential decay components. The primary decay component was fast, and the decay constants of 0.5, 2.5, 5, and 10% Sr-admixed Ce:$CaHfO_3$ were 23.7, 26.7, 21.5, and 21.4 ns, respectively. The secondary decay component was slower than the main decay component, and the decay time constants of 0.5, 2.5, 5, and 10% Sr-admixed Ce:$CaHfO_3$ were 209.8, 209.8, 205.6, and 275.6 ns, respectively. Through the comparison of these decay components with those in previous studies, the origins of the primary and secondary decay components were judged to be the 5d–4f transition of Ce^{3+} and the host material.[31]

Figure 6 shows the afterglow curves of Sr-admixed Ce:$CaHfO_3$ single crystals. The afterglow levels of 0.5, 2.5, 5, and 10% Sr-admixed Ce:$CaHfO_3$ were 222, 792, 136, and 908 ppm, respectively. These values were smaller than those of Ce:$CaHfO_3$ and Mg-admixed Ce:$CaHfO_3$.[31,32] The mechanism of suppression of the afterglow level by Sr admixture is

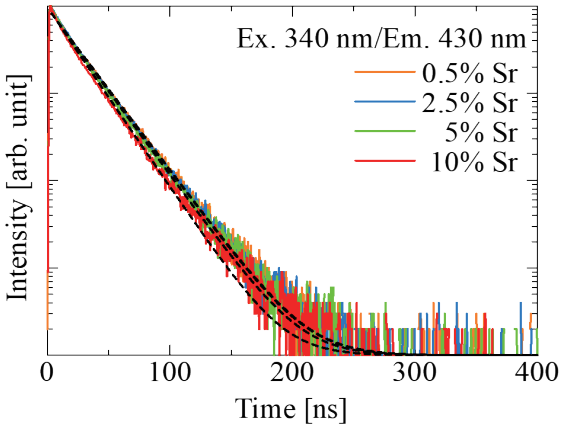

Fig. 3. (Color online) PL decay curves of Sr-admixed Ce:$CaHfO_3$ single crystals.

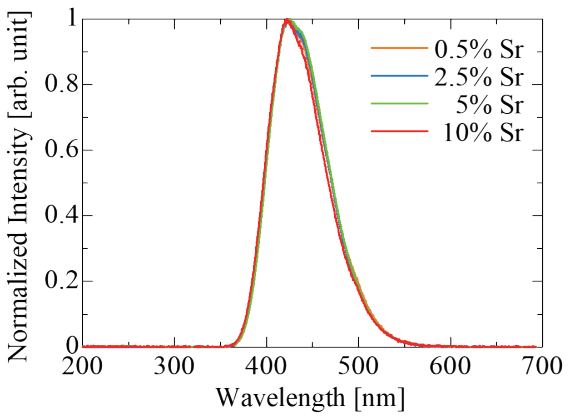

Fig. 4. (Color online) Radioluminescence spectra of Sr-admixed Ce:$CaHfO_3$ single crystals.

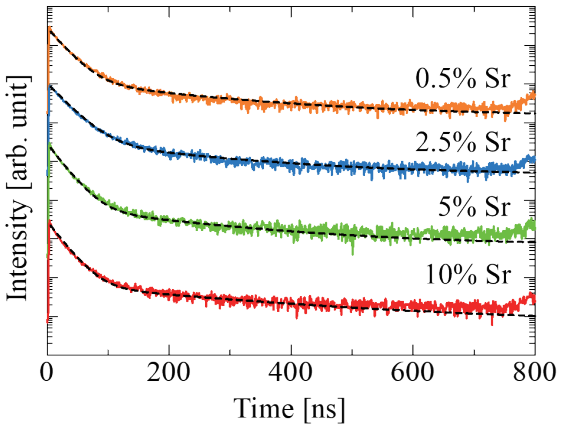

Fig. 5. (Color online) Radioluminescence decay curves of Sr-admixed Ce:$CaHfO_3$ single crystals.

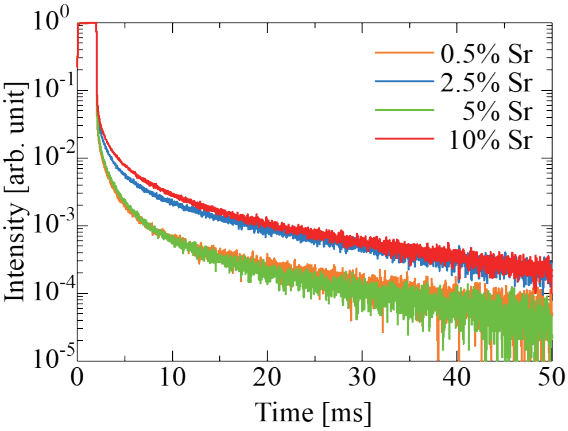

Fig. 6. (Color online) Afterglow curves of Sr-admixed Ce:$CaHfO_3$ single crystals.

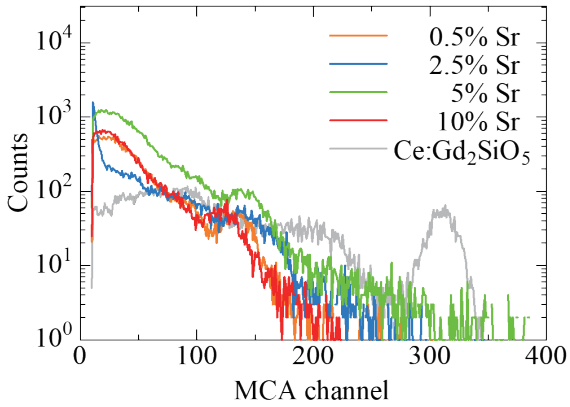

Fig. 7. (Color online) Pulse height distribution of 137Cs γ-ray using Sr-admixed Ce:$CaHfO_3$ single crystals.

unclear in the present study, but a possible reason is the compensation of Ca by Sr. During the synthesis of the Ce:$CaHfO_3$ single crystal, Ca evaporated owing to the high melting point of $CaHfO_3$. The deficiency of Ca may lead to the high afterglow level in $CaHfO_3$. Sr admixture compensates for the deficiency of Ca, leading to the suppression of the afterglow levels. The variation of the afterglow levels may be blamed for the condition of the single crystal growth. Figure 7 shows the pulse height distribution of ^{137}Cs γ-rays using Sr-admixed Ce:$CaHfO_3$ single crystals. The light yields of 0.5, 2.5, 5, and 10% Sr-admixed Ce:$CaHfO_3$ were 2840, 2840, 2880, and 2600 photons/MeV, respectively. These values were lower than those observed in Ce:$CaHfO_3$ and Mg-admixed Ce:$CaHfO_3$.[31,32]

The Mg admix improves the light yield of Ce:$CaHfO_3$. The Sr admix improves the afterglow of Ce:$CaHfO_3$. The ionic radius may affect the light yield of Ce:$CaHfO_3$. To elucidate the admix effect in Ce:$CaHfO_3$, Be- and Ba-admixed Ce:$CaHfO_3$ should be investigated in the future. In addition, the maximum PL QY of these admixed Ce:$CaHfO_3$ was about 57%. To increase the light yield, PL QY must be increased because the light yield depends on PL QY. The Ce^{3+} concentration affects PL QY, and Ce^{4+} may decrease the PL QY of Ce^{3+}. To increase the Ce^{3+}/Ce^{4+} ratio, it is desirable to conduct crystal growth in an inert gas atmosphere.

3. Conclusion

The Sr-admixed Ce:$CaHfO_3$ single crystals were successfully synthesized, and the PL and scintillation properties were investigated. The broad luminescence band was observed at around 430 nm in PL and radioluminescence, and the decay time constant was approximately 23 ns. The origin of luminescence was the 5d–4f transition of Ce^{3+}. The afterglow levels were firmly suppressed by Sr admixture. The deficiency of Ca was compensated by Sr admixture, leading to the suppression for the afterglow levels. The Sr-admixed Ce:$CaHfO_3$ can apply to the integrated-type detection owing to its relatively low afterglow levels.

Acknowledgments

This work was supported by Grants-in-Aid for Early-Carrier Scientists (25K17974) and Scientific Research C (25K06658) from the Japan Society for the Promotion of Science (JSPS) and the Cooperative Research Project of the Research Center for Biomedical Engineering.

References

1 M. Moszyński, J. Zalipska, M. Balcerzyk, M. Kapusta, W. Mengesha, and J. D. Valentine: Nucl. Instrum. Methods Phys. Res. A **484** (2002) 259. https://doi.org/10.1016/S0168-9002(01)01964-7
2 C. W. E. van Eijk: Nucl. Instrum. Methods Phys. Res. A **460** (2001) 1. https://doi.org/10.1016/S0168-9002(00)01088-3
3 C. L. Melcher and J. S. Schweitzer: IEEE Trans. Nucl. Sci. **39** (1992) 502. https://doi.org/10.1109/23.159655
4 S. Shimizu, K. Kurashige, T. Usui, N. Shimura, K. Sumiya, N. Senguttuvan, A. Gunji, M. Kamada, and H. Ishibashi: IEEE Trans. Nucl. Sci. **53** (2006) 14. https://doi.org/10.1109/TNS.2005.862975
5 K. Takagi and T. Fukazawa: Appl. Phys. Lett. **42** (1983) 43. https://doi.org/10.1063/1.93760
6 K. Miyazaki, D. Nakauchi, T. Kato, N. Kawaguchi, and T. Yanagida: Sens. Mater. **36** (2024) 515. https://doi.org/10.18494/SAM4756
7 T. Kunikata, P. Kantuptim, D. Shiratori, T. Kato, D. Nakauchi, N. Kawaguchi, and T. Yanagida: Sens. Mater. **36** (2024) 457. https://doi.org/10.18494/SAM4754
8 K. Ichiba, T. Kato, D. Nakauchi, N. Kawaguchi, and T. Yanagida: Sens. Mater. **36** (2024) 451. https://doi.org/10.18494/SAM4752
9 Y. Endo, K. Ichiba, D. Nakauchi, T. Kato, N. Kawaguchi, and T. Yanagida: Sens. Mater. **36** (2024) 473. https://doi.org/10.18494/SAM4758
10 K. Yamabayashi, K. Okazaki, D. Nakauchi, T. Kato, N. Kawaguchi, and T. Yanagida: Sens. Mater. **36** (2024) 523. https://doi.org/10.18494/SAM4760
11 H. Kimura, H. Fukushima, K. Watanabe, T. Fujiwara, H. Kato, M. Tanaka, T. Kato, D. Nakauchi, N. Kawaguchi, and T. Yanagida: Sens. Mater. **36** (2024) 507. https://doi.org/10.18494/SAM4767
12 K. Okazaki, M. Koshimizu, D. Nakauchi, Y. Takebuchi, K. Ichiba, H. Ezawa, T. Kato, N. Kawaguchi, and T. Yanagida: Sens. Mater. **37** (2025) 557. https://doi.org/10.18494/SAM5427
13 M. Ishida, A. Watanabe, H. Kawamoto, Y. Fujimoto, and K. Asai: Sens. Mater. **37** (2025) 607. https://doi.org/10.18494/SAM5482
14 D. Nakauchi, T. Kato, N. Kawaguchi, and T. Yanagida: Sens. Mater. **37** (2025) 547. https://doi.org/10.18494/SAM5425
15 R. Takahashi, K. Okazaki, D. Nakauchi, T. Kato, N. Kawaguchi, and T. Yanagida: Sens. Mater. **37** (2025) 593. https://doi.org/10.18494/SAM5435
16 T. Kunikata, K. Okazaki, H. Kimura, S. Takase, T. Kato, D. Nakauchi, N. Kawaguchi, and T. Yanagida: Sens. Mater. **37** (2025) 563. https://doi.org/10.18494/SAM5428
17 K. Ichiba, K. Watanabe, K. Okazaki, T. Kato, D. Nakauchi, N. Kawaguchi, and T. Yanagida: Sens. Mater. **37** (2025) 553. https://doi.org/10.18494/SAM5426
18 Y. Endo, K. Ichiba, D. Nakauchi, T. Kato, N. Kawaguchi, and T. Yanagida: Sens. Mater. **37** (2025) 587. https://doi.org/10.18494/SAM5432
19 K. Miyazaki, D. Nakauchi, Y. Takebuchi, T. Kato, N. Kawaguchi, and T. Yanagida: Sens. Mater. **37** (2025) 575. https://doi.org/10.18494/SAM5430
20 T. Kato, D. Nakauchi, N. Kawaguchi, and T. Yanagida: Sens. Mater. **36** (2024) 531. https://doi.org/10.18494/SAM4749
21 H. Fukushima, D. Nakauchi, T. Kato, N. Kawaguchi, and T. Yanagida: Sens. Mater. **36** (2024) 489. https://doi.org/10.18494/SAM4762
22 N. Kawaguchi, K. Yamabayashi, K. Okazaki, R. Takahashi, T. Kato, D. Nakauchi, and T. Yanagida: Sens. Mater. **37** (2025) 617. https://doi.org/10.18494/SAM5479
23 S. Otake, S. Takase, T. Kato, D. Nakauchi, N. Kawaguchi, and T. Yanagida: Sens. Mater. **37** (2025) 519. https://doi.org/10.18494/SAM5433
24 H. Fukushima, R. Tsubouchi, T. Matsuura, T. Yoneda, and T. Yanagida: Sens. Mater. **37** (2025) 487. https://doi.org/10.18494/SAM5438

25 D. Nakauchi, H. Kimura, D. Shiratori, T. Kato, N. Kawaguchi, and T. Yanagida: Sens. Mater. **36** (2024) 573. https://doi.org/10.18494/SAM4750
26 Y. Takebuchi, A. Masuno, D. Shiratori, K. Ichiba, A. Nishikawa, T. Kato, D. Nakauchi, N. Kawaguchi, and T. Yanagida: Sens. Mater. **36** (2024) 579. https://doi.org/10.18494/SAM4751
27 K. Okazaki, D. Nakauchi, A. Nishikawa, T. Kato, N. Kawaguchi, and T. Yanagida: Sens. Mater. **36** (2024) 587. https://doi.org/10.18494/SAM4753
28 D. Shiratori, A. Masuno, T. Kato, Y. Fukuchi, and T. Yanagida: Sens. Mater. **37** (2025) 497. https://doi.org/10.18494/SAM5439
29 S. Muneta, N. Kawano, D. Nakauchi, T. Kato, K. Okazaki, K. Ichiba, T. Kunikata, A. Nishikawa, K. Miyazaki, F. Kagaya, K. Shinozaki, and T. Yanagida: Sens. Mater. **37** (2025) 509. https://doi.org/10.18494/SAM5441
30 K. Miyajima, A. Nishikawa, T. Kato, D. Nakauchi, N. Kawaguchi, and T. Yanagida: Sens. Mater. **37** (2025) 481. https://doi.org/10.18494/SAM5436
31 H. Fukushima, D. Nakauchi, T. Kato, N. Kawaguchi, and T. Yanagida: J. Lumin. **250** (2022) 119088. https://doi.org/10.1016/j.jlumin.2022.119088
32 H. Fukushima, D. Nakauchi, T. Kato, N. Kawaguchi, and T. Yanagida: Sens. Mater. **35** (2023) 429. https://doi.org/10.18494/SAM4139
33 R. D. Shannon: Acta Crystallogr. A **32** (1976) 751. https://doi.org/10.1107/S0567739476001551
34 T. Yanagida, K. Kamada, Y. Fujimoto, H. Yagi, and T. Yanagitani: Opt. Mater. **35** (2013) 2480. https://doi.org/10.1016/j.optmat.2013.07.002
35 T. Yanagida, Y. Fujimoto, T. Ito, K. Uchiyama, and K. Mori: Appl. Phys. Express. **7** (2014) 062401. https://doi.org/10.7567/APEX.7.062401
36 H. Fukushima, D. Nakauchi, G. Okada, N. Kawaguchi, and T. Yanagida: J. Mater. Sci.: Mater. Electron. **29** (2018) 21033. https://doi.org/10.1007/s10854-018-0249-9